

Microwave Dielectric Properties of Bi_2O_3 - TiO_2 Composite Ceramics

Anna-Karin Axelsson, Maladil Sebastian, and Neil McN Alford[†]

Physical Electronics and Materials, South Bank University, London SE1 0AA, UK
(Received March 19, 2003; Accepted March 31, 2003)

ABSTRACT

Bi_2O_3 - TiO_2 composite dielectric ceramics have been prepared by a conventional solid state ceramic route. The composite ceramics were prepared with starting materials of different origin and the microwave dielectric properties were investigated. The sintered ceramics were characterised by X-ray diffraction, scanning electron microscopy, energy dispersive X-ray microanalysis, Raman and microwave methods. Structural and microstructural analyses identified two separate phases: TiO_2 (rutile) and $\text{Bi}_2\text{Ti}_4\text{O}_{11}$. The separate grains of titania and bismuth titanate were distributed uniformly in the ceramic matrix. The composition $0.88\text{TiO}_2\cdot 0.12\text{Bi}_2\text{Ti}_4\text{O}_{11}$ was found to have a $Q \times f$ of 9,300 GHz (measured at a frequency of 3.9 GHz), a temperature coefficient of frequency, τ_{cf} , near zero and a high relative permittivity, ϵ_r , of 83. The microwave dielectric properties were measured down to 20°K. The quality factor increased on cooling the ceramic samples.

Key words : Dielectric ceramics, Microwave material, Bismuth titanate, Bi_2O_3 , TiO_2

1. Introduction

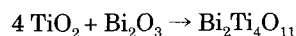
The recent progress in wireless communication and satellite broadcasting has resulted in an increasing demand for dielectric resonators. The important characteristics required for a dielectric resonator material are high relative dielectric constant (ϵ_r) for miniaturisation, high quality factor (Q) for improved selectivity and low temperature variation of resonant frequency (τ_{cf}) for stability. For applications in the mobile phone handset one needs a high ϵ_r in the range 80–100 for miniaturisation. The number of materials available for such applications is somewhat limited. $\text{Ba}(\text{Nd},\text{Sm})_2\text{Ti}_5\text{O}_{14}$ is a favoured composition for commercial use in such applications. However, the quality factor \times frequency product ($Q \times f$) of $\text{Ba}(\text{Nd},\text{Sm})_2\text{Ti}_5\text{O}_{14}$ is limited to about 7000¹⁾ at the microwave frequencies of interest (approximately 1–5 GHz). Hence intensive searches for high ϵ_r and high Q materials are in progress. Recently it has been reported^{2,4)} that mixing the metal oxides TiO_2 and Bi_2O_3 in various ratios can lead to materials with comparatively high ϵ_r with values ranging from 46–95. For example, a series of bismuth titanate ceramics were prepared with $\text{TiO}_2\text{:Bi}_2\text{O}_3$ mol-ratio varying between 1 : 1 to 22 : 1, yielding ϵ_r values between 68–121 (2 MHz). Fukuda *et al.*¹⁾ reported ϵ_r between 53 to 105 with ratios ranging between 4 : 1 to 51 : 1. ϵ_r between 56 to 125 with $\text{TiO}_2\text{:Bi}_2\text{O}_3$ mol-ratio ranging from 2 : 1 to 4.5 : 1 were also obtained. The sintered Bi_2O_3 - TiO_2 ceramics in this report consist of two separate

phases: TiO_2 and $\text{Bi}_2\text{Ti}_4\text{O}_{11}$. The $\text{Bi}_2\text{Ti}_4\text{O}_{11}$ has a ϵ_r of 51 and a negative τ_{cf} of -530 ppm/°K whereas the TiO_2 has $\epsilon_r=100$ with a positive τ_{cf} of $+430$ ppm/°K. The high positive τ_{cf} of TiO_2 can therefore, be compensated by the high negative τ_{cf} of $\text{Bi}_2\text{Ti}_4\text{O}_{11}$. The formation of different bismuth titanate phases depends on the starting composition and on the conditions of the solid-state reaction. Hence in the present paper we have undertaken a detailed study of the effect of different starting materials on the microwave dielectric properties at room temperature and down to 20°K.

2. Experimental

The Bi_2O_3 - TiO_2 composite samples were prepared by a conventional solid-state reaction method using TiO_2 (Degussa P25, purity 99.9%) or (Pi-Kem Ltd, TiO_2 99.9% purity) and Bi_2O_3 (Alfa, 99.9%). The mole ratios of the bismuth titanate composites in the starting powders ($\text{TiO}_2\text{:Bi}_2\text{O}_3$) were 51.63 : 1, 23.39 : 1, 11.34 : 1, and 4.00 : 1.

In the 4 : 1 TiO_2 - Bi_2O_3 ratio, 100% bismuth titanate may be formed according to the following reaction:



Four different sets of powder mixtures were prepared to investigate the importance of starting material and powder preparation on the properties of the final sintered material. The details are given in Table 1.

It has been noted previously that a solid phase reaction between Bi_2O_3 and TiO_2 begins at temperatures above 750°C.³⁾ The precursor Bi_2O_3 is highly volatile and maintaining the desired stoichiometry for the final material becomes very difficult. To study the possibility of reducing the sintering temperature by reducing the particle size and

[†]Corresponding author : Neil McN Alford

E-mail : alfordn@sbu.ac.uk

Tel : +44-(0)-207-815-7559 Fax : +44-(0)-207-815-7599

Table 1. Powder Preparation and Sintering Conditions

Name	Starting material	calcining	Milling	Surface area (m ² /g)	Sintering
Set 1	TiO ₂ (PI-KEM)-Bi ₂ O ₃ (Alfa)	950°C/2 h	24 h ball mill	0.62–1.29	1100–1300°C 2–4 h
Set 2	TiO ₂ (PI-KEM)-Bi ₂ O ₃ (Alfa)	950°C/2 h	600 rpm/3 h	1.01–2.59	1050–1200°C 2–4 h
Set 3	TiO ₂ (DegussaP25)-Bi ₂ O ₃ (Alfa)	950°C/2 h	600 rpm/3 h	1.33–4.35	1050–1200°C 2 h
Set 4	TiO ₂ (Degussa P25)-Bi ₂ O ₃ (Alfa)	None	Only Bi ₂ O ₃ 600 rpm/3 h	32.5–46.22	1050–1200°C 2 h

the impact on the dielectric properties, the same source of precursor powders using different milling procedures were compared in sets 1 and 2. In sets 3 and 4 nanosized Degussa P25 (25% anatase + 75% rutile, approx. 30 nm) was used as a source of TiO₂. The anatase converts irreversibly to the favoured rutile structure at around 700°C. This crystal transition increases the TiO₂ reaction capacity due to the release of free energy.

The powder mixtures, sets 1, 2 and 3 were dry mixed for 5 h before calcination. The calcined powder from set 1 was then milled in deionised water using Partially Stabilised Zirconia (PSZ) balls for 24 h, dried and dry-ball milled again to remove caked agglomerates. A Pulverizette-6 (Fritsch) high energy planetary mill, with a PSZ pot and PSZ balls, was used to comminute set 2 (for comparison with set 1) and 3. In the last set (set 4), we wished to examine the effect of using uncalcined Bi₂O₃ and the TiO₂, however, as the Bi₂O₃ was rather a coarse powder, the Bi₂O₃ was milled using the planetary mill before dry mixing with Degussa P25. This powder set was *not* calcined.

The particle sizes of the different sets of calcined and ball milled powders were measured and compared (see Table 1). Particle size was measured down to 0.04 μm by laser diffraction (Coulter LS). The surface areas of the different sets were measured on a Coulter SA3100 gas adsorption apparatus using N₂ as the adsorption gas. Samples were degassed prior to analysis, and the surface areas were calculated from adsorption/desorption isotherms using the BET method. The equivalent spherical diameter can be calculated from surface area using the following equation:

$$d = \frac{6}{S.A. \times \rho}$$

where d =equivalent spherical diameter, $S.A.$ =surface area, and ρ =density.

The as-prepared powder was uniaxially pressed into pellets by using a 13 mm die at 0.5 MPa before sintering at a range of temperatures between 1050 and 1250°C for 2 h. The dimensions of the final discs were such that the length/diameter ratio was between 0.4 to 0.5.

The structure and phase purity of the composites were monitored by X-ray diffraction analysis using Philips XPert MRD system and with diffractometer PW33. Diffraction patterns were obtained using a CuK_α radiation with a 2θ step size of 0.02° and 2s count time between 15° < 2θ < 90°.

Raman spectra of the samples were obtained with a Renishaw system 2000 microprobe with a 488 nm line of an Ar⁺ laser as exciting radiation with nominally <4.0 mW power

incident on the sample surface. The laser line was focused onto the sample by a cylindrical microscope lens of ×50 magnification with a spot diameter of 3±1 μm. All spectra were taken in a backscattering geometry with polarised incident and scattered light. The 520.5 cm⁻¹ phonon line of silicon was used as a calibration standard. The Raman spectra were taken from the interior of the samples by cutting the sintered samples in half. Bismuth deficiency at the surface was easily observed and it was found that this deficiency was confined to the surface where the characteristic single phase Bi₂Ti₄O₁₁ Raman mode (at approximately 191 cm⁻¹) was well pronounced in the interior of the puck and almost absent at the surface of the puck.

Qualitative and quantitative micro structural measurements were carried out by Scanning Electron Microscopy (SEM; Hitachi 4300) equipped with an Energy Dispersive X-ray Spectrometer (EDXA; Oxford Instruments INCA System).

The resonant frequency (f), ϵ_r and quality factor (Q) were measured by a resonant cavity method by examining the TE₀₁₃ mode using a network analyser (Hewlett Packard 8720D). The sample was placed on a low loss quartz spacer inside an oxygen free high purity copper cavity. The cavity height was adjusted so that the space above the sample was the same as the spacers thickness. The copper cavity containing the dielectric sample was placed on a cold-head inside a closedcycle cooling system (CTI Cryogenics Model 22 refrigerator and 8200 cryo-compressor). This allowed measurement to be made between 15 and 320°K. The temperature was controlled and measured by using a Lakeshore 330 Temperature Controller. The τ_c was evaluated from the temperature variation of the resonant frequency.

3. Results and Discussion

3.1. Sintering and the Effect of Particle size

The four sets of composite samples were sintered to dense (>98% of theoretical density) ceramics.

Sets 1 and 2 were made using the same titania (PiKem Ltd, UK) and Bi₂O₃ source powders but utilising different milling procedures. Sets 2 and 3 were made with Degussa P25 TiO₂. The variation in TiO₂ powder source, calcinations and milling conditions is reflected in the sintering behaviour of the different sets of materials. Fig. 1(a) shows the variation of the optimum sintering temperatures as a function of Bi₂O₃ content. The optimum sintering temperature is that temperature where the Q is maximised and is generally consistent with the temperature at which the maxi-

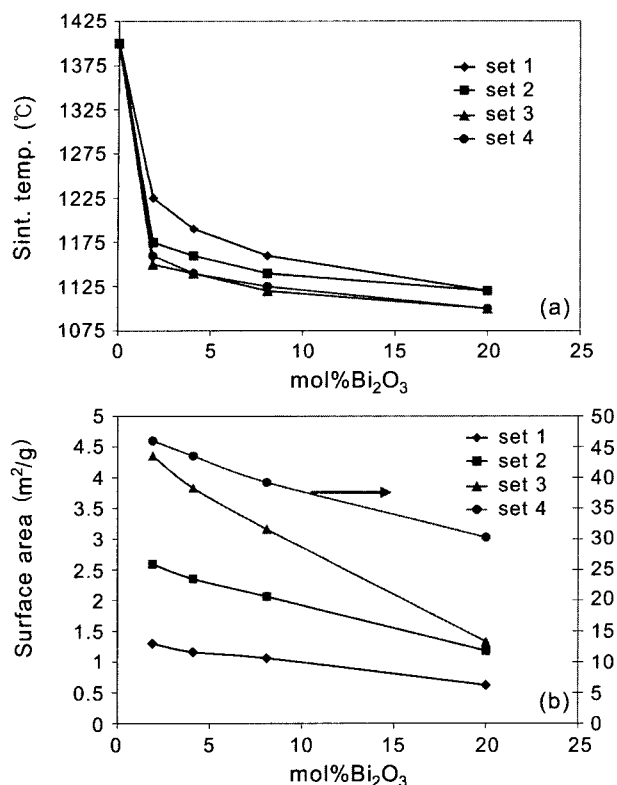


Fig. 1. Optimal sintering temperature for the four sets as a function of added mol% Bi₂O₃ (a) and surface area of the starting powders (b).

imum density is achieved in the ceramic.

The sintering temperature decreased with increasing Bi₂O₃ content. Fig. 1(b) shows the variation in surface area of the particles as a function of Bi₂O₃ content. It is evident from the figure that the high energy planetary ball milled samples in sets 2 and 3 exhibited a finer particle size compared with set 1 milled in a conventional ball mill. The higher surface areas of planetary ball milled powders resulted in a decrease of the optimum sintering temperature (see Fig. 1(a)).

Sets 3 and 4 using nano-sized Degussa P-25 made it possible for significant decrease in the optimum sintering temperature for all composites. In set 4, only the Bi₂O₃ powder was milled and then mixed with powder of TiO₂ (Degussa P25). In this case alone, the mixed powder was *not* calcined and this is reflected in the high surface area of the starting powder.

The approximate particle sizes were 1.0–1.6 μm (Set 1 ballmilled PiKem TiO₂ and Bi₂O₃), 0.6–1.0 μm (set 2 planetary high energy milled PiKem TiO₂ and Bi₂O₃), 0.3–0.7 μm (Set 3 P25 and Bi₂O₃-calcined) and under 100 nm (Set 4 P25 and Bi₂O₃-uncalcined). The small particle size of Degussa P25 TiO₂ results in strong attractive forces between the particles¹ resulting in the formation of agglomerates² ranging between 100–5000 nm. Pure Degussa P25 is difficult to sinter to a dense product partly because the conversion of the anatase to rutile involves a density change (anatase

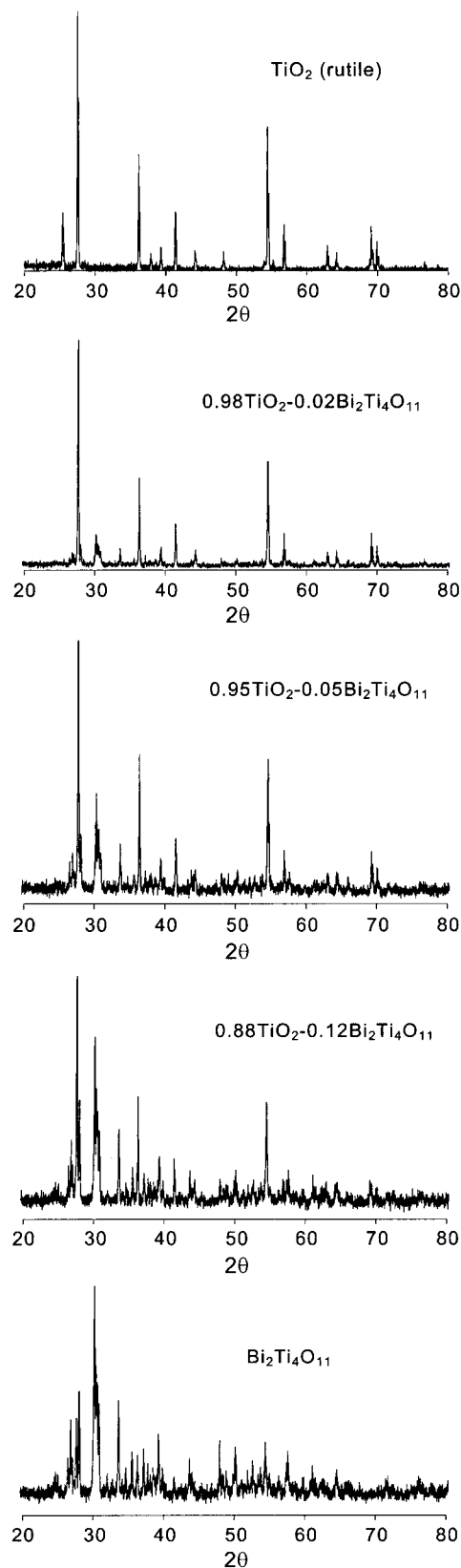


Fig. 2. XRD pattern of TiO₂-Bi₂Ti₄O₁₁ composites showing increasing fraction of the bismuth titanate phase with increased amount of added Bi₂O₃. The final pattern is single phase Bi₂Ti₄O₁₁.

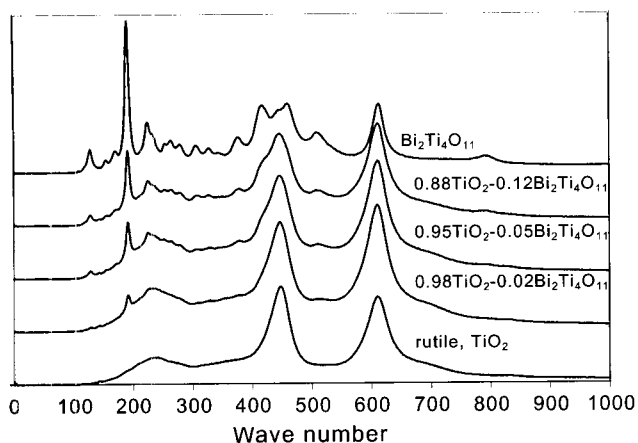


Fig. 3. Raman spectra of titania and bismuth titanate composites as a function of increasing bismuth content showing the development of the two phases, TiO_2 and $\text{Bi}_2\text{Ti}_4\text{O}_{11}$.

3.9 g/cm^3 and rutile 4.2 g/cm^3). But more problematic is the presence of the agglomerates themselves, which introduce backstresses and inhibit sintering.³ It was found that an increased level of low melting point bismuth oxide reduced the effect of these unwanted agglomerates and this is because the backstress is somewhat relieved by the formation of a liquid phase.

3.2. XRD, Raman, and SEM

XRD patterns of the various bismuth titanates composites are shown in Fig. 2. With reference to standard patterns of $\text{Bi}_2\text{Ti}_2\text{O}_7$ (JCPDS No. 32-0118), $\text{Bi}_2\text{Ti}_3\text{O}_{12}$ (JCPDS No. 35-0795), and $\text{Bi}_2\text{Ti}_4\text{O}_{11}$ (JCPDS No. 15-0325), it was concluded that the bismuth titanate phase formed in the process was $\text{Bi}_2\text{Ti}_4\text{O}_{11}$. By introducing more bismuth to the titania, it becomes clear that the bismuth titanate phase co-exists with the titania phase suggesting that two separate phases are present. As reported earlier by Fukuda *et al.*² the composition 4 : 1 of TiO_2 : Bi_2O_3 has an XRD pattern indicating this is single phase $\text{Bi}_2\text{Ti}_4\text{O}_{11}$.

Fig. 3 shows the Raman spectra of $\text{Bi}_2\text{Ti}_4\text{O}_{11}$ - TiO_2 compos-

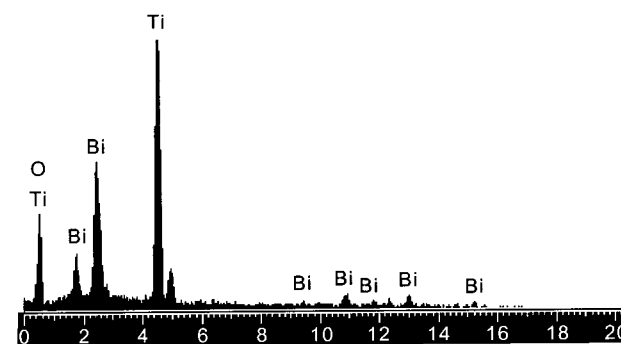


Fig. 5. EDXA spectrum of the 0.88TiO_2 - $0.12\text{Bi}_2\text{Ti}_4\text{O}_{11}$.

ites. The Raman spectra indicate the development of the two phase composite well. In the figure it can be seen that even as the bismuth content increases, the Raman shift of true TiO_2 modes at 446 and 608 cm^{-1} (230 cm^{-1} is a second order mode) remain constant until the last spectra of 4 : 1 of TiO_2 : Bi_2O_3 where single phase of $\text{Bi}_2\text{Ti}_4\text{O}_{11}$ is formed. This finding indicates that the TiO_6 octahedron is intact and that the Ti-O bond angle and/or distances unchanged by the increased amount of bismuth. If no separate phases of titania and bismuth titanate were formed but only single phase of bismuth titanates of different structures, one would expect the Ti-O peaks to shift due to distortions of the lattice. The spectrum was estimated to contain a total of 21 vibration bands in the $\text{Bi}_2\text{Ti}_4\text{O}_{11}$ ceramics reflecting the complex structure formed.

The microstructure of the bismuth titanates was monitored by Scanning Electron Microscopy (Hitachi 4300). Fig. 4(a) shows a micrograph of a sintered and polished sample of the 0.88TiO_2 - $0.12\text{Bi}_2\text{Ti}_4\text{O}_{11}$ composite with near zero τ_{cr} . The Bi and Ti are fairly evenly distributed as seen in the element maps seen in Fig. 4(b) and 4(c).

Fig. 5 is the EDXA spectrum of 0.88TiO_2 - $0.12\text{Bi}_2\text{Ti}_4\text{O}_{11}$. Quantitative analysis from the spectrum in Fig. 5 suggested a ratio of 6 : 1 for Ti:Bi rather than an expected stoichiometry of 5.34 : 1. This can be explained by the bismuth deficiency at the surface and has also been observed by Duran *et al.*⁴

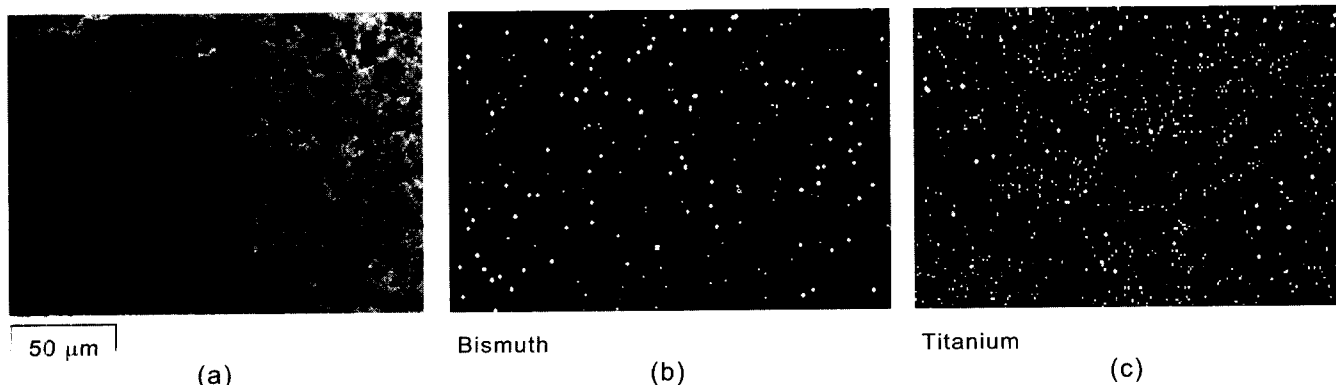


Fig. 4. (a) SEM image of the 0.88TiO_2 - $0.12\text{Bi}_2\text{Ti}_4\text{O}_{11}$ composite, (b) EDXA distribution map for Bi, and (c) distribution map for Ti. The distribution of both Ti and Bi is fairly uniform.

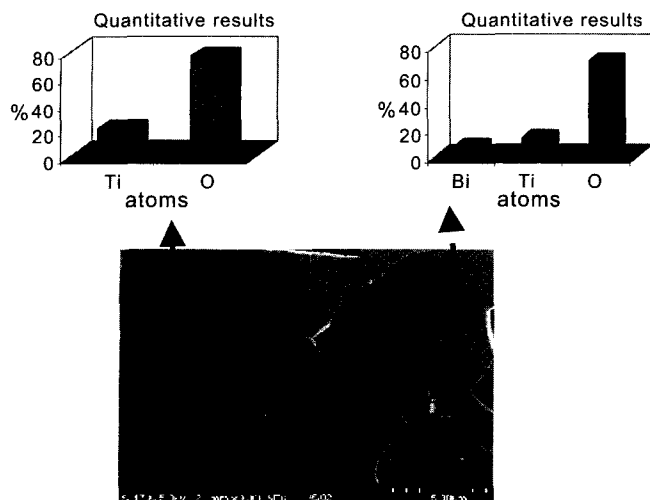


Fig. 6. SEM image and quantitative analysis confirming the presence of two separate phases, bismuth titanate and TiO_2 in a sintered $0.88\text{TiO}_2\text{-}0.12\text{Bi}_2\text{Ti}_4\text{O}_{11}$ material.

Fig. 6 show how individual grains of bismuth titanate and titanium oxide exist as two separate phases in the $0.88\text{TiO}_2\text{-}0.12\text{Bi}_2\text{Ti}_4\text{O}_{11}$ composite. The darker grains belong to titanium oxide and the lighter to the bismuth titanate.

3.3. Dielectric Properties

The Q , ϵ_r , and frequency were studied over a temperature range of 25–320 °K. Table 2 shows the microwave dielectric properties for each set for samples measured at room temperature. All the results in Table 2 were for samples with relative density around 98%. The main anomaly is the unexpectedly low values for the $Q \times f$ of $0.98\text{TiO}_2\text{-}0.02\text{Bi}_2\text{Ti}_4\text{O}_{11}$ in sets 2 and 3 ($Q \times f = 9000$ and 8000 GHz, respectively) compared with $Q \times f = 18000$ GHz for sets 1 and 4. We have no clear explanation for this anomaly. For the low τ_{cf} composition ($0.88\text{TiO}_2\text{-}0.12\text{Bi}_2\text{Ti}_4\text{O}_{11}$) the $Q \times f$ ranges between 6500–9300 GHz. In all sets the ϵ_r decreased with increasing amount of $\text{Bi}_2\text{Ti}_4\text{O}_{11}$ content as expected.

The temperature coefficient of frequency calculated as $d(f)/d(T)/T_n$ was positive for all composites except the single phase bismuth titanate. The variation of τ_{cf} as a function of fractional TiO_2 can be seen in Fig. 7. The τ_{cf} gradually reduces to a value of 3 ppm/K at a composition $0.88\text{TiO}_2\text{-}0.12\text{Bi}_2\text{Ti}_4\text{O}_{11}$. In Table 1, the value for dense Pi-Kem TiO_2 is included for completeness.

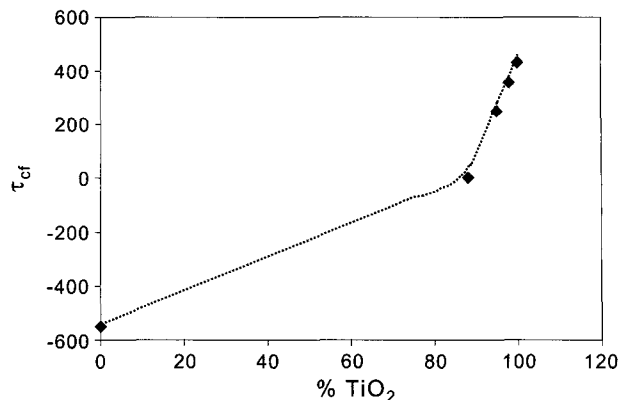


Fig. 7. τ_{cf} as a function of TiO_2 content.

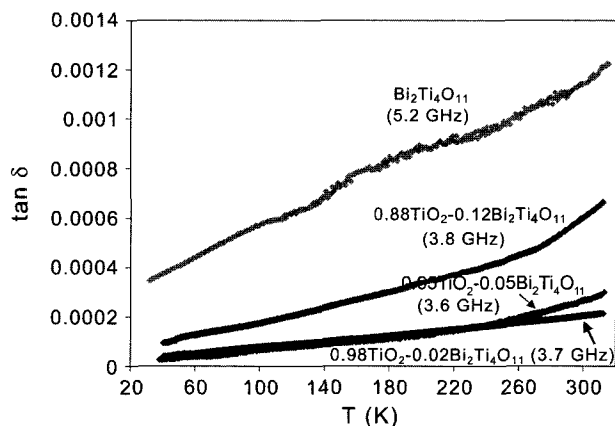


Fig. 8. Dielectric loss ($\tan \delta$) over temperature for the for different composites in set 4.

Fig. 8 shows the temperature dependence of the loss for the four compositions taken from set 4. The $\tan \delta$ vs temperature profile can be a good indicator of the quality of a Ti bearing ceramic as any slight reduction from Ti^{4+} to Ti^{3+} produces marked differences in the temperature behaviour of the $\tan \delta$.⁵⁾ The behaviour is indicative of well oxygenated material as we do not observe any serious anomalies in the curves. In materials where there is oxygen deficiency for example, we would expect a high value for the loss extending to approximately 70°K where the loss suddenly reduces suggestive of carrier freeze-out. This is observed in pure TiO_2 ceramics that are slightly oxygen deficient.⁸⁾

Table 2. Microwave Dielectric Properties of the Composites

Composite	Set 1				Set 2			Set 3			Set 4		
	ρ_{th} ($\text{g}\cdot\text{cm}^{-3}$)	$Q \times f$ (GHz)	ϵ_r	τ_{cf} (ppm/°K)	$Q \times f$ (GHz)	ϵ_r	τ_{cf} (ppm/°K)	$Q \times f$ (GHz)	ϵ_r	τ_{cf} (ppm/°K)	$Q \times f$ (GHz)	ϵ_r	τ_{cf} (ppm/°K)
TiO_2	4.26	50,000	100	430									
$0.98 \text{TiO}_2\text{-}0.02\text{Bi}_2\text{Ti}_4\text{O}_{11}$	4.3	18000	95	351	9000	94	390	8000	94	335	18000	95	355
$0.95 \text{TiO}_2\text{-}0.05\text{Bi}_2\text{Ti}_4\text{O}_{11}$	4.6	11200	88	268	9700	89	238	11200	93	254	12500	84	230
$0.88 \text{TiO}_2\text{-}0.12\text{Bi}_2\text{Ti}_4\text{O}_{11}$	5.0	6500	81	15	7000	81	8	8500	81	8	9300	74	3
$\text{Bi}_2\text{Ti}_4\text{O}_{11}$	5.9	4800	47	-540	4500	52	-550	4900	53	-547	4900	46	-520

4. Conclusions

Bi₂Ti₄O₁₁-TiO₂ composite dielectric resonator samples were prepared using powders from different sources and by employing different processing conditions. It was found that the microwave dielectric properties were very much dependent on the starting powders and the processing conditions. In this study we found that by mixing nanosized TiO₂ (Degussa P-25) with milled Bi₂O₃ and avoiding a calcination step, a dense ceramic composite was obtained that displayed good microwave dielectric properties with Q×f=9300 GHz, τ_c=3 ppm/°K, and ε_r=74.

Microstructural analysis by using XRD, Raman, SEM, and EDXA revealed the presence of two separate phases, TiO₂ and Bi₂Ti₄O₁₁, in all of the final composites.

The dielectric loss decreased on cooling the samples and this indicates that there are few residual Ti³⁺ species in the composite and that the material is well oxygenated.

Acknowledgement

The author would like to acknowledge EPSRC and Framework V.

REFERENCES

1. R. Uvic, I. M. Reaney, and W. E. Lee, *Int. Mater. Rev.*, **43** [5] 205-19 (1998).
2. K. Fukuda, R. Kitoh, and I. Awai, "Microwave Characteristics of TiO₂-Bi₂O₃ Dielectric Resonator," *Jpn. J. of App. Phy.*, **32** 4584-88 (1993).
3. S. P. Yordanov, CH. P. Carapanov, I. S. Ivanov, and P. T. Cholakov, "Dielectric Properties of Ferroelectric Bi₂Ti₃O₉ Ceramics," *Ferroelectrics*, **209** 541-52 (1998).
4. N. McN Alford, J. D. Birchall, and K. Kendall, "High Strength Ceramics through Colloidal Control to Remove Defects," *Nature*, **330** [6143] 51-5 (1987).
5. N. McN Alford, J. D. Birchall, and K. Kendall, "Engineering Ceramics The Process Problem," *Mats. Sci. & Technol.*, **2** 329-36 (1986).
6. W. J. Clegg, N. McN Alford, and J. D. Birchall, "Back Stresses and the Sintering of Composites," *Brit. Ceram. Proc.*, **39** 247 (1987).
7. P. Duran, C. Moure, M. Villegas, J. Tartaj, A. C. Cabaalero, and J. F. Fernandez," *J. Am. Ceram. Soc.*, **83** [5] 1029-32 (2000).
8. A. Templeton, X. Wang, S. J. Penn, S. J. Webb, L. F. Cohen, and N. McN Alford, "Microwave Dielectric Loss of Titanium Oxide," *J. Am. Ceram. Soc.*, **83** [1] 95-100 (2000).